JCI insight

Sustained inhibition of NPY/AgRP neuronal activity by FGF1

Eunsang Hwang, … , Kevin W. Williams, Michael W. Schwartz

JCI Insight. 2022. https://doi.org/10.1172/jci.insight.160891.

Research In-Press Preview Endocrinology Neuroscience

In rodent models of type 2 diabetes (T2D), central administration of fibroblast growth factor 1 (FGF1) normalizes elevated blood glucose levels in a manner that is sustained for weeks or months. Increased activity of NPY/AgRP neurons in the hypothalamic arcuate nucleus (ARC) is implicated in the pathogenesis of hyperglycemia in these animals, and the ARC is a key brain area for the antidiabetic action of FGF1. We therefore sought to determine whether FGF1 inhibits NPY/AgRP neurons, and if so whether this inhibitory effect is sufficiently durable to offer a feasible explanation for sustained diabetes remission induced by central administration of FGF1. Here we show that FGF1 inhibits ARC NPY/AgRP neuron activity, both after icv injection in vivo and when applied ex vivo in a slice preparation, and that the underlying mechanism involves increased input from presynaptic GABAergic neurons. Following central administration, the inhibitory effect of FGF1 on NPY/AgRP neurons is also highly durable, lasting for at least two weeks. To our knowledge, no precedent for such a prolonged inhibitory effect exists. Future studies are warranted to determine whether NPY/AgRP neuron inhibition contributes to the sustained antidiabetic action elicited by icv FGF1 injection in rodent models of T2D.

Sustained inhibition of NPY/AgRP neuronal activity by FGF1

Eunsang Hwang[1,7], Jarrad M. Scarlett[2,3,7], Arian F. Baquero[4], Camdin M. Bennett[4], Yanbin Dong[1], Dominic Chau[1], Jenny M. Brown[2,5], Aaron J. Mercer[4], Thomas H. Meek[4,6], Kevin L. Grove[4], Bao Anh Phan[2], Gregory J. Morton[2], Kevin W. Williams[1,**], Michael W. Schwartz[2,*]

[1] Center for Hypothalamic Research, Department of Internal Medicine, the University of Texas Southwestern Medical Center at Dallas, Dallas, TX, USA.

[2] University of Washington Medicine Diabetes Institute, Department of Medicine, Seattle, WA, 98109, USA.

[3] Department of Pediatric Gastroenterology and Hepatology, Seattle Children's Hospital, Seattle, WA, 98145, USA.

[4] Obesity Research, Novo Nordisk Research Center Seattle, Seattle, WA 98109

[5] University of Copenhagen, Novo Nordisk Foundation Center for Basic Metabolic Research, Copenhagen, DK-2200, Denmark.

[6] Discovery Technologies & Genomics, Novo Nordisk Research Center Oxford, Oxford, OX3 7FZ, United Kingdom

[7] These authors are co-first authors.

** Corresponding author. University of Texas Southwestern Medical Center at Dallas, 5323 Harry Hines Boulevard, Dallas, TX, 75390-9077, USA. E-mail: kevin.williams@ utsouthwestern.edu (K.W. Williams).

* Corresponding author. University of Washington Medicine Diabetes Institute, 750 Republican Street, Box 358062, Seattle, WA, 98109, USA. E-mail: mschwart@uw.edu (M.W. Schwartz).

ABSTRACT

In rodent models of type 2 diabetes (T2D), central administration of fibroblast growth factor 1 (FGF1) normalizes elevated blood glucose levels in a manner that is sustained for weeks or months. Increased activity of NPY/AgRP neurons in the hypothalamic arcuate nucleus (ARC) is implicated in the pathogenesis of hyperglycemia in these animals, and the ARC is a key brain area for the antidiabetic action of FGF1. We therefore sought to determine whether FGF1 inhibits NPY/AgRP neurons, and if so whether this inhibitory effect is sufficiently durable to offer a feasible explanation for sustained diabetes remission induced by central administration of FGF1. Here we show that FGF1 inhibits ARC NPY/AgRP neuron activity, both after icv injection in vivo and when applied ex vivo in a slice preparation, and that the underlying mechanism involves increased input from presynaptic GABAergic neurons. Following central administration, the inhibitory effect of FGF1 on NPY/AgRP neurons is also highly durable, lasting for at least two weeks. To our knowledge, no precedent for such a prolonged inhibitory effect exists. Future studies are warranted to determine whether NPY/AgRP neuron inhibition contributes to the sustained antidiabetic action elicited by icv FGF1 injection in rodent models of T2D.

INTRODUCTION

In addition to its role as a tissue growth factor involved in functions ranging from brain development to angiogenesis, fibroblast growth factor 1 (FGF1) exerts a highly durable glucose-lowering action following central administration in rodent models of type 2 diabetes (T2D) (1-3). In particular, a single intracerebroventricular (icv) injection of FGF1 induces remission of diabetic hyperglycemia lasting for weeks or even months in both mouse (*Lep*$^{ob/ob}$ and *LepR*$^{db/db}$) and rat (Zucker Diabetic Fatty; ZDF) models of T2D. The mediobasal hypothalamus (MBH) is a key brain area involved in glucose homeostasis that is highly responsive to FGF1 following icv injection (4). Moreover, the effect of icv FGF1 injection to elicit sustained remission of diabetic hyperglycemia can be recapitulated by microinjection of a much lower FGF1 dose directly into the MBH (4), implicating this brain area in the mechanism underlying sustained glucose lowering following icv FGF1 administration.

The arcuate nucleus (ARC) is situated adjacent to the floor of the 3rd ventricle in the MBH. The ARC contains two neuron subsets with opposing effects on energy balance that interact to determine the activity of the hypothalamic melanocortin system. On the one hand are neurons that co-express agouti-related peptide (AgRP) and neuropeptide Y (henceforth referred to as NPY/AgRP neurons) that when activated, reduce signaling via the melanocortin 4 receptor (Mc4r) (AgRP is an inverse agonist of this receptor). Opposing this action are adjacent neurons that express pro-opiomelanocortin (POMC) and release α-melanocyte stimulating hormone (α-MSH), a ligand that binds to and activates Mc4r (5, 6). Under usual circumstances, the activity of these two neuronal subsets is reciprocally regulated such that when NPY/AgRP neurons are activated, POMC neurons are inhibited and vice-versa. In states of negative energy balance (e.g., fasting), for example, NPY/AgRP

neuron activation combines with POMC neuron inhibition to potently reduce Mc4r signaling and thereby promote a state of positive energy balance leading to recovery of lost weight.

Glucose metabolism is also impaired by NPY/AgRP neuron activation (7-12), while conversely, blood glucose, food intake and body weight are each reduced when NPY/AgRP neurons are silenced or ablated, including in mouse models of T2D (13-15). Since elevated hypothalamic *Agrp* and *Npy* mRNA levels are a characteristic finding in rodent models of diabetes (16), we wondered whether NPY/AgRP neuron inhibition might be a target for the antidiabetic action of FGF1 in the MBH. Support for this hypothesis includes evidence from 3 different mouse models of T2D showing that sustained glucose lowering induced by icv FGF1 injection is blocked when Mc4r signaling is disrupted by either genetic or pharmacological means (16). These findings suggest that for FGF1 to exert its central antidiabetic action, melanocortin signaling must increase, and this can only happen by inhibiting NPY/AgRP neurons, activating POMC neurons, or some combination of the two (5, 6).

Consistent with this notion is recent evidence from the Kievit lab showing that in an ex vivo brain slice preparation, POMC neurons are depolarized following bath application of FGF1 (1, 2, 17), and additional findings implicate NPY/AgRP neurons as targets for the action of FGF1 as well. Specifically, a study in diabetic *Lep*$^{ob/ob}$ mice demonstrated that at the transcriptional level NPY/AgRP neurons are the most FGF1-responsive hypothalamic neuronal cell type (16), and further that both *Npy* and *Agrp* mRNA expression are reduced for weeks following a single icv FGF1 injection, suggestive of a sustained inhibitory response (16). Another line of evidence involves perineuronal nets (PNNs), extracellular matrix specializations that enmesh and thereby regulate the function of distinct neuronal subsets across many brain areas. We recently reported that most NPY/AgRP neurons are enmeshed by PNNs (18), and subsequently that these PNNs are depleted in the in ZDF rat model of T2D (19). Moreover, these ARC PNNs are a reassembled following icv FGF1 injection, and this restorative effect of FGF1 appears to be required for sustained diabetes remission to be induced in these animals (19).

Multiple convergent findings therefore support a model whereby FGF1 action in the MBH increases melanocortin signaling, at least in part by inhibiting NPY/AgRP neurons. In the current work, we combined histochemical and electrophysiological tools to investigate effects of FGF1 on NPY/AgRP neuron function both in wild-type (WT) mice and in NPY/AgRP-reporter mice that were crossed onto the *Lep*$^{ob/ob}$ mouse background, enabling us to identify and target NPY/AgRP neurons for electrophysiological recordings in a highly FGF1-responsive mouse model of T2D. To assess the onset and duration of the response of these neurons to FGF1, studies were carried out both acutely and 2 weeks after icv injection.

RESULTS

Acute FGF1 administration inhibits NPY/AgRP neurons

As a first step to investigate whether NPY/AgRP neurons are inhibited by the action of FGF1, we utilized transgenic *Agrp*$^{Cre:GFP}$ mice to enable colocalization of cFos protein, a marker of neuron activation, in labelled NPY/AgRP neurons. This study was performed in non-diabetic mice that were fasted for 24 h to increase baseline expression of cFos in NPY/AgRP neurons. Mice were euthanized 90 min after icv injection of either vehicle or FGF1 (3 µg), with representative images from treated animals presented in (Figure 1A,B). Although the total number of AgRP+ neurons was comparable across all mice tested (Figure 1C), we found the total number of both cFos+ cells and cFos+/AgRP+ neurons across the entire rostral to caudal extent of the ARC was markedly reduced in fasted mice receiving icv FGF1 injection compared to saline-injected controls (Figure 1D,E). These findings suggest that in fasted normal mice, AgRP neurons are rapidly inhibited following icv FGF1 administration, in agreement with our prior observation that icv FGF1 decreases hypothalamic *Agrp* and *Npy* mRNA levels (16).

We then examined the response of NPY/AgRP neurons to bath application of FGF1 *ex vivo* using whole-cell patch-clamp electrophysiology in non-diabetic C57Bl6 mice (in which the neurons are marked by GFP expressed under the control of the *Npy* promoter (20)). When K^+ was used as the major cation in the recording pipette, the resting membrane potential (RMP) of ARC NPY/AgRP neurons was -43.7 ± 0.5 mV. Bath application of FGF1 (10 nM in aCSF) hyperpolarized the membrane potential in 5 of 13 NPY neurons (38.5% of NPY neurons targeted, p=0.0009; Figure 2A) in a dose responsive manner (Supplementary Figure 1). In the subset of these neurons that were also active (baseline firing rate ≥ 0.5 Hz), we observed a progressive decrease in the frequency of action potentials over time (n=4, p=0.0205 @ 14 min; p=0.0135 @ 15 min; p=0.0088 @ 16 min; p=0.0069 @ 17 min; p=0.0065 @ 18 min; one-way ANOVA, Figure 2B). Cumulatively, the overall membrane potential from all NPY/AgRP neurons, including responsive and non-responsive cells, was significantly hyperpolarized in response to

FGF1 bath application (n=13; p=0.038 paired t test; Figure 2A). Interestingly, antagonism of GABAergic neurotransmission prevented the hyperpolarization of NPY/AgRP neurons (Figure 2C), in agreement with our finding of increased GABAergic synaptic transmission during acute FGF1 administration (Supplementary figure 2). Together, these findings suggest that FGF1 inhibits NPY/AgRP neurons indirectly via a mechanism requiring increased GABAergic input.

Sustained inhibition of NPY/AgRP neurons following icv FGF1 administration to NPY^{hrGFP}::*Lep$^{ob/ob}$* mice

Next, we determined whether sustained diabetes remission induced by icv FGF1 administration is associated with a persistent decrease in the activity of arcuate NPY/AgRP neurons. In this experiment, we used whole-cell patch clamp electrophysiological recordings on NPY neurons from male NPY^{hrGFP}::*Lep$^{ob/ob}$* and *Lep$^{ob/+}$* mice. Based on previous reports describing long-lasting hypothalamic effects following icv FGF1 administration in mice (1, 2, 17), these studies were performed two weeks after a single icv injection of either saline or FGF1 (3 µg). As expected based on our previous observations (2, 3), *Lep*$^{ob/ob}$ mice receiving FGF1 (3 µg, icv) exhibited transient reductions of food intake and body weight that returned to baseline within days after injection, whereas no such effects were observed in *Lep$^{ob/ob}$* mice receiving icv saline (Supplementary figure 3). Also consistent with earlier reports (21), NPY/AgRP neurons from obese, diabetic *Lep$^{ob/ob}$* mice receiving icv saline trended toward an increased AP frequency (Figure 3H) compared to non-obese, non-diabetic *Lep$^{ob/+}$* mice receiving icv saline (p=0.07, Supplementary figure 4H), despite the absence of a similar trend in RMP between groups (p=0.18, Supplementary figure 4G). Moreover, we observed that 2 wk following a single icv FGF1 injection (3 µg), both RMP and AP frequency of NPY/AgRP neurons from *Lep$^{ob/ob}$* mice were significantly decreased compared to values from NPY/AgRP neurons of *Lep$^{ob/ob}$* mice receiving icv saline (RMP: $t(43) = 2.021$, $p = 0.0495$; AP Frequency: $t(43) = 2.091$, $p = 0.0424$;

Figure 3H). It is noteworthy that the AP frequency of NPY/AgRP neurons measured 2 wk after icv FGF1 treatment in *Lep*$^{ob/ob}$ mice was comparable to values observed in icv saline-treated, non-diabetic *Lep*$^{ob/+}$ mice. Stated differently, it appears that elevated baseline NPY/AgRP activity in these mice is normalized for at least 2 wk following a single icv injection of FGF1.

These findings collectively demonstrate that the increased activity of NPY/AgRP neurons in the *Lep*$^{ob/ob}$ mouse model of T2D is reversed at least 2 wk following icv injection of a single dose of FGF1 that reliably elicits sustained reversal of hyperglycemia in these animals (1, 2, 4). The remarkably long-lived duration of this inhibitory effect is compatible with a role for reduced NPY/AgRP neuron activity in the effect of FGF1 to induce sustained diabetes remission in *Lep*$^{ob/ob}$ mice, although additional studies are needed to test this hypothesis directly.

FGF1 enhances GABAergic tone in NPY/AgRP neurons from *Lep*$^{ob/ob}$ mice

Based on our finding that the acute effect of FGF1 to inhibit ARC NPY/AgRP neurons requires GABAergic synaptic transmission (Figure 2C), we next asked whether a similar mechanism contributes to the sustained inhibition of these neurons in *Lep*$^{ob/ob}$ mice. To address this question, we monitored inhibitory and excitatory postsynaptic activity of NPY/AgRP neurons from NPY^{hrGFP}::*Lep*$^{ob/ob}$ and *Lep*$^{ob/+}$ mice two weeks after injection of either saline or FGF1 (3 µg, icv). Similar to previous reports in juvenile mice (22), ARC NPY/AgRP neurons from *Lep*$^{ob/ob}$ mice receiving icv saline exhibited an increase in excitatory input (Figure 4C) while also receiving less inhibitory input (Figure 4G) when compared to *Lep*$^{ob/+}$ mice (Supplementary figure 5C, G). These changes in synaptic activity were independent of changes in amplitude (Figure 4D, H and Supplementary figure 5D, H) and putatively contributed to the higher AP frequency in the former animals (Figure 3H and Supplementary figure 4H).

While excitatory and inhibitory synaptic activity of NPY/AgRP neurons was not altered 2 weeks after icv FGF1 (3 µg) in *Lep*$^{ob/+}$ mice (Supplementary figure 5), the frequency of inhibitory

input to NPY/AgRP neurons from *Lep*$^{ob/ob}$ mice was increased following FGF1 administration (3 µg FGF1, icv; $t(38) = 2.839$, $p = 0.0072$, Figure 4G), while the amplitude remained unchanged ($t(38) = 0.3869$, $p = 0.7010$, Figure 4H). The frequency and amplitude of excitatory synaptic activity to NPY/AgRP neurons from *Lep*$^{ob/ob}$ mice 2 weeks after icv FGF1 injection was also unaltered when compared to mice receiving saline (EPSC frequency; $t(40) = 1.213$, $p = 0.2322$, EPSC amplitude; $t(40) = 0.600$, $p = 0.5515$, Figure 4C and D). Together, these findings demonstrate that the long-lasting inhibitory effect of icv FGF1 administration on NPY/AgRP neuron activity is associated with (and putatively mediated by) increased GABAergic input onto these neurons, with no detectable change in excitatory input. This interpretation is also consistent with evidence that mRNA encoding FGF receptor 1 is expressed in only ~20% of NPY/AgRP neurons (123/644 total neurons, Supplementary figure 6), implying a non-cell autonomous mechanism underlying FGF1-induced inhibition of at least some of these neurons.

DISCUSSION

In the current study, we report that in non-diabetic WT mice, the activity of NPY/AgRP neurons is rapidly reduced both following icv FGF1 injection in vivo (based on cFos expression in fasted mice) and after bath application of FGF1 in an ex vivo brain slice preparation (based on electrophysiological assessments). Perhaps more importantly, we also show that in the *Lep*$^{ob/ob}$ mouse model of T2D, NPY/AgRP neuronal activity remains inhibited for at least 2 wk following a single icv injection of FGF1 (relative to icv vehicle-injected controls) and further, that the underlying mechanism involves increased synaptic input from upstream GABAergic neurons. The unprecedented duration of this inhibitory effect makes it attractive as a potential mediator of sustained glucose lowering elicited by centrally administered FGF1, and future studies are warranted to test this hypothesis.

In normal mice, NPY/AgrRP neuron activity is subject to regulation by distinct nutrient-related signals that operate over multiple time scales (23-28). The most rapidly conveyed afferent input is simply the sight or smell of food, which in a fasted animal can inhibit NPY/AgRP neurons within seconds. Beyond this, afferent signals generated by the GI tract in response to nutrient ingestion act over an intermediate time scale (minutes to hours), whereas humoral signals generated in proportion to body fat mass and energy balance (such as insulin and leptin) provide a less dynamic and more continuous source of inhibitory tone (23, 26). The net effect of these various inhibitory inputs is that NPY/AgRP neurons tend to be relatively inactive unless/until the animal experiences a state of negative balance sufficient to threaten body fuel stores. In this setting, activation of NPY/AgRP neurons is both necessary and sufficient for the hyperphagic response that promotes positive energy balance and replenishes depleted fuel stores (29).

Under pathological conditions, however, activation of these neurons can cause both obesity and diabetes, and hyperactivity of these neurons is a common feature in rodent models of T2D

(21). In diabetic *Lep*$^{ob/ob}$ mice, for example, NPY/AgRP neuron activity is increased compared to nondiabetic WT controls (21), a finding confirmed in the current study. Moreover, the reduction of melanocortin signaling that results from excessive NPY/AgRP neuron activity in these animals is implicated in their obese, diabetic phenotype (30). Conversely, glucose homeostasis can be improved in diabetic animals by restoring intact melanocortin signaling (16, 31-33).

Based on these findings, increased melanocortin signaling is an attractive candidate mediator of the sustained antidiabetic action elicited by FGF1. Consistent with this notion, the MBH is both a crucial brain area for this FGF1 effect (3) and the principal area controlling melanocortin system tone. Moreover, hypothalamic levels of *Npy* and *Agrp* mRNA are reduced for up to 6 weeks following a single icv FGF1 injection in *Lep*$^{ob/ob}$ mice (16). Based on these considerations, we sought to determine if NPY/AgRP neurons are inhibited by FGF1 and if so, whether the effect is sufficiently prolonged to qualify as a candidate mediator of FGF1's sustained antidiabetic action. In support of this hypothesis, we report that these neurons are rapidly inhibited by FGF1 both in vivo and ex vivo, and that in diabetic *Lep*$^{ob/ob}$ mice, this effect persists for at least 2 weeks following icv FGF1 injection (16). Highly durable inhibition of NPY/AgRP neurons likely contributes to the increased melanocortin signaling implicated in sustained diabetes remission induced by the central action of FGF1 (16).

In addition to their finding that bath application of FGF1 depolarizes POMC neurons in an ex vivo slice preparation (also predicted to increase melanocortin signaling), recent work from the Kievet laboratory indicates that FGF1 fails to consistently inhibit NPY/AgRP neurons (34). While the latter finding appears incongruent with the current results, we note that this assessment was based on analyses of these neurons as a population. When the response of individual NPY/AgRP neurons is considered, however, the number inhibited by FGF1 (34) is consistent with our own data. These findings suggest that NPY/AgRP neurons are not a monolithic population with respect to the response to FGF1, and raise the possibility that rather than acting

on NPY/AgRP neurons themselves, the primary effect of FGF1 is on an upstream neuronal population that synapses onto NPY/AgRP neurons.

Consistent with this interpretation is our finding that FGF1-induced inhibition of NPY/AgRP neurons ex vivo is blocked by bath application of a GABAergic antagonist, implying that at least some effects of FGF1 on NPY/AgRP neurons are mediated indirectly. Further support for this hypothesis is provided by evidence that whereas FGF receptors are highly expressed by glial cell types (35), *Fgfr1* mRNA is expressed by only a small fraction (~20%) of NPY/AgRP neurons. Moreover, blood glucose levels are minimally impacted when FGFR1 is selectively deleted from NPY/AgRP neurons (36). While additional studies are necessary to identify upstream GABAergic neurons and establish their contribution to the inhibitory effect of FGF1 on NPY/AgRP neurons, we note that at the transcriptional level, glial cells – astrocytes and tanycytes in particular – are far more FGF1-responsive than are neurons (16). Combined with evidence that evidence that cellular contacts between astrocytes and NPY/AgRP neurons increase markedly following icv FGF1 injection in $Lep^{ob/ob}$ mice (16), the possibility is raised that FGF1 action on glial cells contributes to the sustained inhibition of NPY/AgRP neurons that we observed. This hypothesis is also compatible with evidence of a role for PNNs in the response to FGF1, as most NPY/AgRP neurons are enmeshed by PNNs (18), and the abundance of these PNNs is reduced in the ARC of obese, diabetic ZDF rats. Furthermore, not only does icv FGF1 injection restore these PNNs to normal, but intact PNNs appear to be required for sustained normalization of glycemia by icv FGF1 in these animals (19). Yet another piece of the puzzle of FGF1 action involves the mitogen-activated protein kinase-extracellular signal-regulated kinase (MAPK-ERK) signal transduction pathway, which is required for proper neuron and glial function (37). This pathway is robustly activated in the MBH following icv FGF1 injection, and this activation lasts at least 24 h (3). Further, pharmacological blockade of this MAPK-ERK activation blocks sustained diabetes remission following icv FGF1 injection in

Lep$^{ob/ob}$ mice (3). These findings collectively indicate that sustained remission of diabetic hyperglycemia following central FGF1 administration is dependent sustained increases of melanocortin signaling, MAPK-ERK signal transduction, glial cell activation and PNN reassembly in the MBH (3). Determining precisely where the highly durable inhibition of NPY/AgRP neurons fits into the sequence of events initiated by FGF1 is an important scientific priority.

The hypothesis that the inhibitory effect of FGF1 on NPY/AgRP neurons involves activation of GABAergic neurons that lie upstream is consistent with a large literature on the control of NPY/AgRP neuron activity (38-44). As one example, the rapid inhibition of NPY/AgRP neurons by food sensory cues is mediated by a subset of GABAergic neurons situated in the ventral aspect of the dorsomedial nucleus (DMN) that synapse onto NPY/AgRP neurons (38, 39, 42). While it is possible that these DMN neurons are direct targets for the action of FGF1, another possibility is that in T2D, loss of PNN enmeshment has a destabilizing effect on synaptic input onto NPY/AgRP neurons, thus reducing tonic inhibition by GABAergic DMN neurons. In this scenario, the restorative effect of FGF1 on these PNNs could in theory help to reestablish inhibitory synaptic input onto NPY/AgRP neurons in a manner that can be sustained over time. Studies to test this hypothesis are underway.

In summary, we report that ARC NPY/AgRP neurons are inhibited following FGF1 administration both in vivo and ex vivo. This inhibitory effect is sustained for at least 2 wk following a single icv FGF1 injection in the *Lep*$^{ob/ob}$ mouse model of T2D, and the underlying mechanism appears to involve increased inhibitory input from presynaptic GABAergic neurons. The highly durable nature of this inhibitory effect, combined with evidence linking NPY/AgRP neuron activation to the pathogenesis of hyperglycemia in diabetic animals, offers a novel, feasible and testable mechanism to explain sustained glucose-lowering elicited by icv FGF1 injection in murine models of T2D. Studies that test this hypothesis are a priority moving forward.

METHODS

Animals

All animal procedures were performed according to the National Institutes of Health Guide for the Care and Use of Laboratory Animals and approved by the Institutional Animal Care and Use Committees at the University of Washington, Novo Nordisk Research Center Seattle, or University of Texas. All animals were housed individually under specific pathogen-free conditions in a temperature-controlled environment (12 h lights on/off cycle; lights on at 7:00 am) with *ad libitum* access to water and standard laboratory chow (LabDiet, St Louis, MO). C57BL/6J, NPY^{hrGFP} and *Lep$^{ob/ob}$* (B6.Cg-Lep^{ob}/J) mice were purchased from Jackson Laboratory (Bar Harbor, ME). Male *Agrp$^{Cre:GFP}$* knock-in mice (version 2, v2) were generated by Dr. Richard Palmiter (29). To identify NPY/AgRP neurons from *Lep$^{ob/ob}$* and wildtype mice for electrophysiological recordings, NPY^{hrGFP} mice (20) were mated to *Lep$^{ob/ob}$* (B6.Cg-Lep^{ob}/J) mice to generate NPY^{hrGFP}::*Lep$^{ob/ob}$* mice (45).

Cannulation surgeries

Lateral ventricle (LV) cannulations (8IC315GAS5SC, 26-ga, Plastics One, Roanoke, VA) were performed under isoflurane anesthesia using the following stereotaxic coordinates: -0.7 mm posterior to bregma; 1.3 mm lateral, and 1.95 mm below the skull surface. Mice were treated peri-operatively with Buprenorphine SR (1 mg/mL; 0.1 mL SQ per 25 g; 1 dose for 72 hours) and Carprofen (1.3 mg/mL; 0.3 mL SQ per 25 g; 1 dose per 24 hours; 3 days) and were allowed to recover for two weeks prior to being studied.

Intracerebroventricular injection

Mean levels of blood glucose and body weight were matched between groups before icv injections. Animals received a single 3 µL icv injection of either murine FGF1 (1 µg/µL; a generous gift from Novo Nordisk) or 0.9% saline using a 33-gauge needle (Plastics One,

Roanoke, VA) extending 0.8 mm beyond the tip of the LV cannula. For chronic studies, body weight and food intake measurements were taken every morning at 10 AM (CST) for three days before injection and daily up to 2 weeks after injection.

Immunofluorescence

Dual-immunofluorescence histochemistry was performed to assess the effect of central administration of FGF1 on fasting-induced cFos induction in NPY/AgRP neurons. *Agrp*$^{Cre:GFP}$ mice underwent lateral ventricular cannulation followed by a 2-week period of recovery and habituation to daily handling. Habituated animals were then fasted for 24 h and received a single icv injection of either Vehicle or FGF1 (3 µg). Ninety minutes later, mice were anesthetized with ketamine and xylazine and perfused with ice-cold phosphate-buffered saline (PBS) followed by 4% paraformaldehyde in 0.1M PBS, after which brains were removed. Anatomically-matched free-floating coronal sections (30 µm thickness) from the rostral to caudal extent of the hypothalamus were collected, washed in PBS at room temperature, permeabilized in 0.1 % Triton X-100 and 0.1% BSA, blocked in freshly prepared 5% normal serum (Jackson ImmunoResearch Laboratories, West Grove, Pennsylvania) and incubated overnight at 4°C with rabbit anti-cFos antibody (1:100,000; PC38; Oncogene Research Products, Boston, MA), followed by incubation in donkey anti-rabbit Alexa 555 (1:1,000; Molecular Probes, Inc., Eugene, OR). Sections were washed, re-blocked in normal serum, and then incubated with chicken anti-GFP antibody (1:5,000; ab13970; Abcam, Cambridge, MA), followed by incubation in goat anti-chicken Alexa 488 (1:1,000; Molecular Probes, Inc., Eugene, OR). Sections were then washed overnight in PBS and mounted on super-frost plus microscope slides. Immunofluorescence images were captured using a Leica SP8X Scanning Confocal microscope (Buffalo Grove, IL) with a HC FLUOTAR L 25X/0.95 W objective. Quantification of total ARC AgRP and cFos cell count was performed using Qupath https://qupath.github.io. Quantification of co-localization of cFos with Agrp neurons was performed by: (i) exporting Qupath images to

ImageJ (Fiji, NIH) and converting to binary images, (ii) using image calculator to multiply matched binary images to identify AgRP neurons that contain cFos, and (iii) quantification of Agrp neurons that were cFos positive was performed using analyze particles feature (46).

Duplex In-Situ Hybridization

Mouse brains were prepared and stained as described previously (Hultman et al. J Comp Neurol 2019). Briefly, mice were deeply anesthetized with ketamine and xylazine, and were transcardially perfused with ice cold 4% PFA, and brains were extracted and post-fixed overnight in 10% neutral buffered formalin. Tissues were subsequently paraffin processed, embedded in Surgiplast paraffin (Leica, Buffalo Grove, IL), sectioned at 5 µm intervals, and placed on to SuperFrost Plus glass slides (Fisher Scientific, Pittsburgh, PA). Each slide included two sections of ARC separated by 750 µm, and we stained ARC pairs from four individual animals. Slides were stained on a Ventana Discovery ULTRA (Ventana Medical Systems, Tucson, AZ) with RNAscope reagents (Advanced Cell Diagnostics, Newark, CA), following technical bulletin #323300-USM-ULT. NPY mRNA was labeled with teal HRP using mouse-specific oligonucleotide probes (Mm-NPY, #313329, Advanced Cell Diagnostics), followed by staining of FGFR1 with fast red (Mm-FGFR1-O1-C2, #454949-C2, Advanced Cell Diagnostics) and a hematoxylin counterstain. Slides were coverslipped using EcoMount (Biocare, Pacheco, CA) and imaged at 20x on an AxioScan.Z1 (Zeiss AG, Oberkochen, Germany). Post-hoc analysis was performed in ImageJ (NIH, Bethesda, MD) to quantify the number of dual positive cells across samples. Our inclusion criteria for dual positive cells had to include 1) visible nuclear staining with hematoxylin, 2) a minimum of 5 dots per perinuclear region of NPY, and 3) a minimum of 1 visible red dot to denote FGFR1 mRNA.

Brain slice preparation

To assess both the acute response of NPY/AgRP neurons to FGF1 ex vivo and activity of these neurons in *Lep*$^{ob/ob}$ mice 2 wk after icv FGF1 injection, brain slices were prepared from mice in which GFP is expressed under the control of the *Npy* promotor (NPY^{hrGFP} mice), as previously described (40, 41, 47-49). Briefly, male mice were deeply anesthetized with i.p. injection of 7% chloral hydrate and transcardially perfused with a modified ice-cold artificial CSF (aCSF) (described below), or high-sucrose aCSF (in mM: 208 sucrose, 2 KCL, 26 $NaHCO_3$, 10 glucose, 1.25 NaH_2PO_4, 2 $MgSO_4$, 1 $CaCl_2$ and 10 HEPES, PH 7.3 ~310 mOsm). The mice were then decapitated, and the entire brain was removed and immediately submerged in ice-cold, carbogen-saturated (95% O_2 and 5% CO_2) aCSF (124-126 mM NaCl, 2.8-5 mM KCl, 1.2 mM $MgCl_2$ or 2 $MgSO_4$, 1-2.5 mM $CaCl_2$, 1.25-2.6 mM NaH_2PO_4, 0-26 mM $NaHCO_3$, 0-10 HEPES, and 5-10 mM glucose. As the sagittal length of arcuate is approximately 1 mm, coronal sections were cut at 250 μm intervals to obtain 4 slices for recording from 1 mouse. Brain sections were made using a Leica VT1000S Vibratome and then incubated in oxygenated aCSF (32 °C–34 °C) for at least 1 h before recording. The slices were bathed in oxygenated aCSF (32 °C–34 °C) at a flow rate of ~1.6 ml/min. All electrophysiology recordings were performed at room temperature.

Whole-cell recordings

The pipette solution for whole-cell recordings was as follows: 125 mM K-gluconate, 2-10 mM KCl, 10 mM HEPES, 5-10 mM EGTA, 1 mM $CaCl_2$, 1 mM $MgCl_2$, and 1-2 mM MgATP, 0-5 HEPES, 0.03 mM Alexa Fluor 350 hydrazide dye, pH 7.3 for NPY^{hrGFP}::*Lep*$^{ob/ob}$. K-gluconate was replaced with equimolar Cs-gluconate for recording of spontaneous IPSCs in response to acute FGF1 administration. Electrophysiological recordings were performed similar to previous reports (40, 41, 50). Briefly, epifluorescence was used to target fluorescent cells, at which time the light source was switched to infrared differential interference contrast imaging to obtain the whole-cell recording (Zeiss Axioskop FS2 Plus equipped with a fixed stage and a

QuantEM:512SC electron-multiplying charge-coupled device camera). Electrophysiological signals were recorded using an Axopatch 700B amplifier (Molecular Devices); low-pass filtered at 2–5 kHz and analyzed offline on a PC with patch-clamp (pCLAMP) electrophysiology data acquisition and analysis program (Molecular Devices). Membrane potentials and firing rates were determined from NPY neurons in brain slices. For acute drug administration, we targeted an NPY/AgRP neuron in 1 slice, and after recording switched to another slice to target the next NPY/AgRP neuron. Recording electrodes showed resistances of 2.5–5 MΩ when filled with the K-gluconate internal solution. Input resistance (IR) was assessed by measuring voltage deflection at the end of the response to a hyperpolarizing rectangular current pulse step (500 ms of −10 to −50 pA). Frequency and peak amplitude of excitatory and inhibitory currents were analyzed by using the Easy electrophysiology program (Easy Electrophysiology Ltd).

Analysis and statistics

For immunohistochemical experiments, data are shown as dot plots representing data from individual animals and bar graphs representing average ± SEM. Statistical analyses using unpaired Student's t-test was performed using R. For bath application studies: A change in membrane potential was required to be at least 2 mV in amplitude, and a change in activity was defined as a ≥25% change in action potential frequency that occurred in response to drug application. Membrane potential values were not compensated to account for junction potential (−8 mV). Effects of FGF1 on spontaneous IPSC frequency before and during acute FGF1 application were analyzed within a recording using the Kolmogorov-Smirnov (K-S) test (a nonparametric, distribution-free goodness-of-fit test for probability distributions). All graphs and figures were generated using either GraphPad Prism 9.0 software (Graphpad Software Inc), or CorelDraw X8 (Corel Corp). All data from different groups were analyzed using an unpaired, paired, or multiple unpaired 2-tailed Student's *t* test as well as 1-way ANOVA where appropriate. Results are reported as the mean ± SEM unless indicated otherwise, as indicated

in each figure legend; where n represents the number of cells studied. Significance was set at *$p < 0.05$ for all statistical measures.

Study approval.

Study approval. All experiments were performed in accordance with the guidelines established by the Guide for the Care and Use of Laboratory Animals (National Academies Press, 2011) and were approved by The University of Texas Institutional Animal Care and Use Committee.

AUTHOR CONTRIBUTIONS

Author order was determined with the following considerations. E.H. contributed most to this study and, therefore, is listed first. E.H., J.M.S., A.F.B., A.M., T.M., G.J.M., K.W.W. and M.W.S. designed the experiments. E.H., J.M.S., A.F.B., Y.D., D.C., J.M.B., A.M., and B.A.P. collected and analyzed the data. E.H., J.M.S., A.F.B., A.M., K.W.W., and M.W.S. wrote the manuscript. All authors reviewed and edited the manuscript. K.W.W. and M.W.S. are the guarantors of this work and thus had full access to all the data in the study and take responsibility for the integrity of the data and the accuracy of the data analysis.

ACKNOWLEDGMENT

The authors gratefully acknowledge Dr. Richard Palmiter (University of Washington) for providing the AgRP-Cre:GFP mice, and Dr. Peilin Chen (Novo Nordisk Research Center Seattle) for executing the automated ISH staining. This work was supported by grants to: E.H. (National Research Foundation of Korea – NRF 2021R1A6A3A14044733), J.M.S. (K08 DK114474, R03 DK128383, and DoD W81XWH2110635), G.J.M. (R01 DK089056, R01 DK124238 and ADA 1-19-IBS-192), K.W.W. (R01 DK119169 and PO1 DK119130-03), and M.W.S (R01 DK101997 and R01 DK083042). J.M.B. was supported by National Heart, Lung, and Blood Institute T32 training grant HL-007312 and the Diabetes Research Center Samuel and Althea Stroum Endowed Graduate Fellowship at the University of Washington.

CONFLICT OF INTEREST

A.F.B., C.M.B., A.J.M, and T.H.M. are employees of Novo Nordisk, which manufactures and sells therapeutics for the treatment of diabetes and obesity. Funding in support of these studies was provided to M.W.S. by Novo Nordisk (CMS-431104).

References Cited

1. Scarlett JM, Muta K, Brown JM, Rojas JM, Matsen ME, Acharya NK, et al. Peripheral Mechanisms Mediating the Sustained Antidiabetic Action of FGF1 in the Brain. *Diabetes.* 2019;68(3):654-64.
2. Scarlett JM, Rojas JM, Matsen ME, Kaiyala KJ, Stefanovski D, Bergman RN, et al. Central injection of fibroblast growth factor 1 induces sustained remission of diabetic hyperglycemia in rodents. *Nat Med.* 2016;22(7):800-6.
3. Brown JM, Bentsen MA, Rausch DM, Phan BA, Wieck D, Wasanwala H, et al. Role of hypothalamic MAPK/ERK signaling and central action of FGF1 in diabetes remission. *iScience.* 2021;24(9):102944.
4. Brown JM, Scarlett JM, Matsen ME, Nguyen HT, Secher A, Jorgensen R, et al. The Hypothalamic Arcuate Nucleus-Median Eminence Is a Target for Sustained Diabetes Remission Induced by Fibroblast Growth Factor 1. *Diabetes.* 2019;68(5):1054-61.
5. Williams KW, and Elmquist JK. From neuroanatomy to behavior: central integration of peripheral signals regulating feeding behavior. *Nat Neurosci.* 2012;15(10):1350-5.
6. Schwartz MW, and Porte D, Jr. Diabetes, obesity, and the brain. *Science.* 2005;307(5708):375-9.
7. Steculorum SM, Ruud J, Karakasilioti I, Backes H, Engstrom Ruud L, Timper K, et al. AgRP Neurons Control Systemic Insulin Sensitivity via Myostatin Expression in Brown Adipose Tissue. *Cell.* 2016;165(1):125-38.
8. Uner AG, Kecik O, Quaresma PGF, De Araujo TM, Lee H, Li W, et al. Role of POMC and AgRP neuronal activities on glycaemia in mice. *Sci Rep.* 2019;9(1):13068.
9. Cavalcanti-de-Albuquerque JP, Bober J, Zimmer MR, and Dietrich MO. Regulation of substrate utilization and adiposity by Agrp neurons. *Nat Commun.* 2019;10(1):311.
10. Krashes MJ, Koda S, Ye C, Rogan SC, Adams AC, Cusher DS, et al. Rapid, reversible activation of AgRP neurons drives feeding behavior in mice. *J Clin Invest.* 2011;121(4):1424-8.
11. Betley JN, Cao ZF, Ritola KD, and Sternson SM. Parallel, redundant circuit organization for homeostatic control of feeding behavior. *Cell.* 2013;155(6):1337-50.
12. Aponte Y, Atasoy D, and Sternson SM. AGRP neurons are sufficient to orchestrate feeding behavior rapidly and without training. *Nat Neurosci.* 2011;14(3):351-5.
13. Gropp E, Shanabrough M, Borok E, Xu AW, Janoschek R, Buch T, et al. Agouti-related peptide-expressing neurons are mandatory for feeding. *Nat Neurosci.* 2005;8(10):1289-91.
14. Wu Q, Boyle MP, and Palmiter RD. Loss of GABAergic signaling by AgRP neurons to the parabrachial nucleus leads to starvation. *Cell.* 2009;137(7):1225-34.
15. Konner AC, Janoschek R, Plum L, Jordan SD, Rother E, Ma X, et al. Insulin action in AgRP-expressing neurons is required for suppression of hepatic glucose production. *Cell Metab.* 2007;5(6):438-49.
16. Bentsen MA, Rausch DM, Mirzadeh Z, Muta K, Scarlett JM, Brown JM, et al. Transcriptomic analysis links diverse hypothalamic cell types to fibroblast growth factor 1-induced sustained diabetes remission. *Nat Commun.* 2020;11(1):4458.
17. Tennant KG, Lindsley SR, Kirigiti MA, True C, and Kievit P. Central and Peripheral Administration of Fibroblast Growth Factor 1 Improves Pancreatic Islet Insulin Secretion in Diabetic Mouse Models. *Diabetes.* 2019;68(7):1462-72.
18. Mirzadeh Z, Alonge KM, Cabrales E, Herranz-Perez V, Scarlett JM, Brown JM, et al. Perineuronal Net Formation during the Critical Period for Neuronal Maturation in the Hypothalamic Arcuate Nucleus. *Nat Metab.* 2019;1(2):212-21.
19. Alonge KM, Mirzadeh Z, Scarlett JM, Logsdon AF, Brown JM, Cabrales E, et al. Hypothalamic perineuronal net assembly is required for sustained diabetes remission induced by fibroblast growth factor 1 in rats. *Nat Metab.* 2020;2(10):1025-33.

20. van den Pol AN, Yao Y, Fu LY, Foo K, Huang H, Coppari R, et al. Neuromedin B and gastrin-releasing peptide excite arcuate nucleus neuropeptide Y neurons in a novel transgenic mouse expressing strong Renilla green fluorescent protein in NPY neurons. *J Neurosci.* 2009;29(14):4622-39.
21. Takahashi KA, and Cone RD. Fasting induces a large, leptin-dependent increase in the intrinsic action potential frequency of orexigenic arcuate nucleus neuropeptide Y/Agouti-related protein neurons. *Endocrinology.* 2005;146(3):1043-7.
22. Pinto S, Roseberry AG, Liu H, Diano S, Shanabrough M, Cai X, et al. Rapid rewiring of arcuate nucleus feeding circuits by leptin. *Science.* 2004;304(5667):110-5.
23. Beutler LR, Corpuz TV, Ahn JS, Kosar S, Song W, Chen Y, et al. Obesity causes selective and long-lasting desensitization of AgRP neurons to dietary fat. *eLife.* 2020;9.
24. Deem JD, Faber CL, and Morton GJ. AgRP neurons: Regulators of feeding, energy expenditure, and behavior. *FEBS J.* 2021.
25. Goldstein N, McKnight AD, Carty JRE, Arnold M, Betley JN, and Alhadeff AL. Hypothalamic detection of macronutrients via multiple gut-brain pathways. *Cell Metab.* 2021;33(3):676-87 e5.
26. Lieu L, Chau D, Afrin S, Dong Y, Alhadeff AL, Betley JN, et al. Effects of metabolic state on the regulation of melanocortin circuits. *Physiol Behav.* 2020;224:113039.
27. Su Z, Alhadeff AL, and Betley JN. Nutritive, Post-ingestive Signals Are the Primary Regulators of AgRP Neuron Activity. *Cell Rep.* 2017;21(10):2724-36.
28. Chen Y, Lin YC, Kuo TW, and Knight ZA. Sensory detection of food rapidly modulates arcuate feeding circuits. *Cell.* 2015;160(5):829-41.
29. Deem JD, Faber CL, Pedersen C, Phan BA, Larsen SA, Ogimoto K, et al. Cold-induced hyperphagia requires AgRP neuron activation in mice. *Elife.* 2020;9.
30. Krashes MJ, Shah BP, Koda S, and Lowell BB. Rapid versus delayed stimulation of feeding by the endogenously released AgRP neuron mediators GABA, NPY, and AgRP. *Cell Metab.* 2013;18(4):588-95.
31. Cowley MA, Pronchuk N, Fan W, Dinulescu DM, Colmers WF, and Cone RD. Integration of NPY, AGRP, and melanocortin signals in the hypothalamic paraventricular nucleus: evidence of a cellular basis for the adipostat. *Neuron.* 1999;24(1):155-63.
32. Graham M, Shutter JR, Sarmiento U, Sarosi I, and Stark KL. Overexpression of Agrt leads to obesity in transgenic mice. *Nat Genet.* 1997;17(3):273-4.
33. Ollmann MM, Wilson BD, Yang YK, Kerns JA, Chen Y, Gantz I, et al. Antagonism of central melanocortin receptors in vitro and in vivo by agouti-related protein. *Science.* 1997;278(5335):135-8.
34. Roberts BL, Kim EJ, Lindsley SR, Tennant KG, and Kievit P. Fibroblast Growth Factor-1 Activates Neurons in the Arcuate Nucleus and Dorsal Vagal Complex. *Front Endocrinol (Lausanne).* 2021;12:772909.
35. Hultman K, Scarlett JM, Baquero AF, Cornea A, Zhang Y, Salinas CBG, et al. The central fibroblast growth factor receptor/beta klotho system: Comprehensive mapping in Mus musculus and comparisons to nonhuman primate and human samples using an automated in situ hybridization platform. *J Comp Neurol.* 2019;527(12):2069-85.
36. Liu S, Marcelin G, Blouet C, Jeong JH, Jo YH, Schwartz GJ, et al. A gut-brain axis regulating glucose metabolism mediated by bile acids and competitive fibroblast growth factor actions at the hypothalamus. *Mol Metab.* 2018;8:37-50.
37. Asih PR, Prikas E, Stefanoska K, Tan ARP, Ahel HI, and Ittner A. Functions of p38 MAP Kinases in the Central Nervous System. *Front Mol Neurosci.* 2020;13:570586.
38. Berrios J, Li C, Madara JC, Garfield AS, Steger JS, Krashes MJ, et al. Food cue regulation of AGRP hunger neurons guides learning. *Nature.* 2021;595(7869):695-700.

39. Garfield AS, Shah BP, Burgess CR, Li MM, Li C, Steger JS, et al. Dynamic GABAergic afferent modulation of AgRP neurons. *Nat Neurosci.* 2016;19(12):1628-35.
40. Dong Y, Carty J, Goldstein N, He Z, Hwang E, Chau D, et al. Time and metabolic state-dependent effects of GLP-1R agonists on NPY/AgRP and POMC neuronal activity in vivo. *Mol Metab.* 2021;54:101352.
41. He Z, Gao Y, Lieu L, Afrin S, Cao J, Michael NJ, et al. Direct and indirect effects of liraglutide on hypothalamic POMC and NPY/AgRP neurons - Implications for energy balance and glucose control. *Mol Metab.* 2019;28:120-34.
42. Xu J, Bartolome CL, Low CS, Yi X, Chien CH, Wang P, et al. Genetic identification of leptin neural circuits in energy and glucose homeostases. *Nature.* 2018;556(7702):505-9.
43. Dicken MS, Tooker RE, and Hentges ST. Regulation of GABA and glutamate release from proopiomelanocortin neuron terminals in intact hypothalamic networks. *J Neurosci.* 2012;32(12):4042-8.
44. Stincic TL, Grachev P, Bosch MA, Ronnekleiv OK, and Kelly MJ. Estradiol Drives the Anorexigenic Activity of Proopiomelanocortin Neurons in Female Mice. *eNeuro.* 2018;5(4).
45. Coleman DL. Effects of parabiosis of obese with diabetes and normal mice. *Diabetologia.* 1973;9(4):294-8.
46. Grishagin IV. Automatic cell counting with ImageJ. *Anal Biochem.* 2015;473:63-5.
47. Mani BK, Puzziferri N, He Z, Rodriguez JA, Osborne-Lawrence S, Metzger NP, et al. LEAP2 changes with body mass and food intake in humans and mice. *J Clin Invest.* 2019;129(9):3909-23.
48. Baquero AF, de Solis AJ, Lindsley SR, Kirigiti MA, Smith MS, Cowley MA, et al. Developmental switch of leptin signaling in arcuate nucleus neurons. *J Neurosci.* 2014;34(30):9982-94.
49. Torz LJ, Osborne-Lawrence S, Rodriguez J, He Z, Cornejo MP, Mustafa ER, et al. Metabolic insights from a GHSR-A203E mutant mouse model. *Mol Metab.* 2020;39:101004.
50. He Z, Gao Y, Alhadeff AL, Castorena CM, Huang Y, Lieu L, et al. Cellular and synaptic reorganization of arcuate NPY/AgRP and POMC neurons after exercise. *Mol Metab.* 2018;18:107-19.

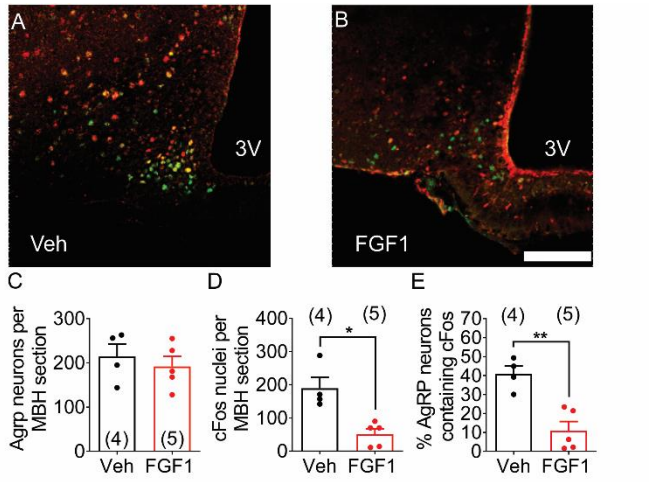

Figure 1. FGF1 inhibits fasting-induced activation of NPY/AgRP neurons. Immunohistochemical detection of AgRP:GFP (green), cFos (red), and colocalization of GFP and cFos in the ARC of 24 hr fasted *Agrp*$^{Cre:GFP}$ mice 90 min after icv Veh or FGF1 (3 µg). Representative coronal image from (A) Veh-treated and (B) FGF1-treated mice. Quantitation of (C) total number of NPY/Agrp neurons, (D) total number of cFos+ cells, and (E) percent of NPY/AgRP neurons that co-express cFos. Scale bar = 100 µm, n = 4–5 group, mean ± SEM. Unpaired t-test, **p<0.01. 3V – third ventricle.

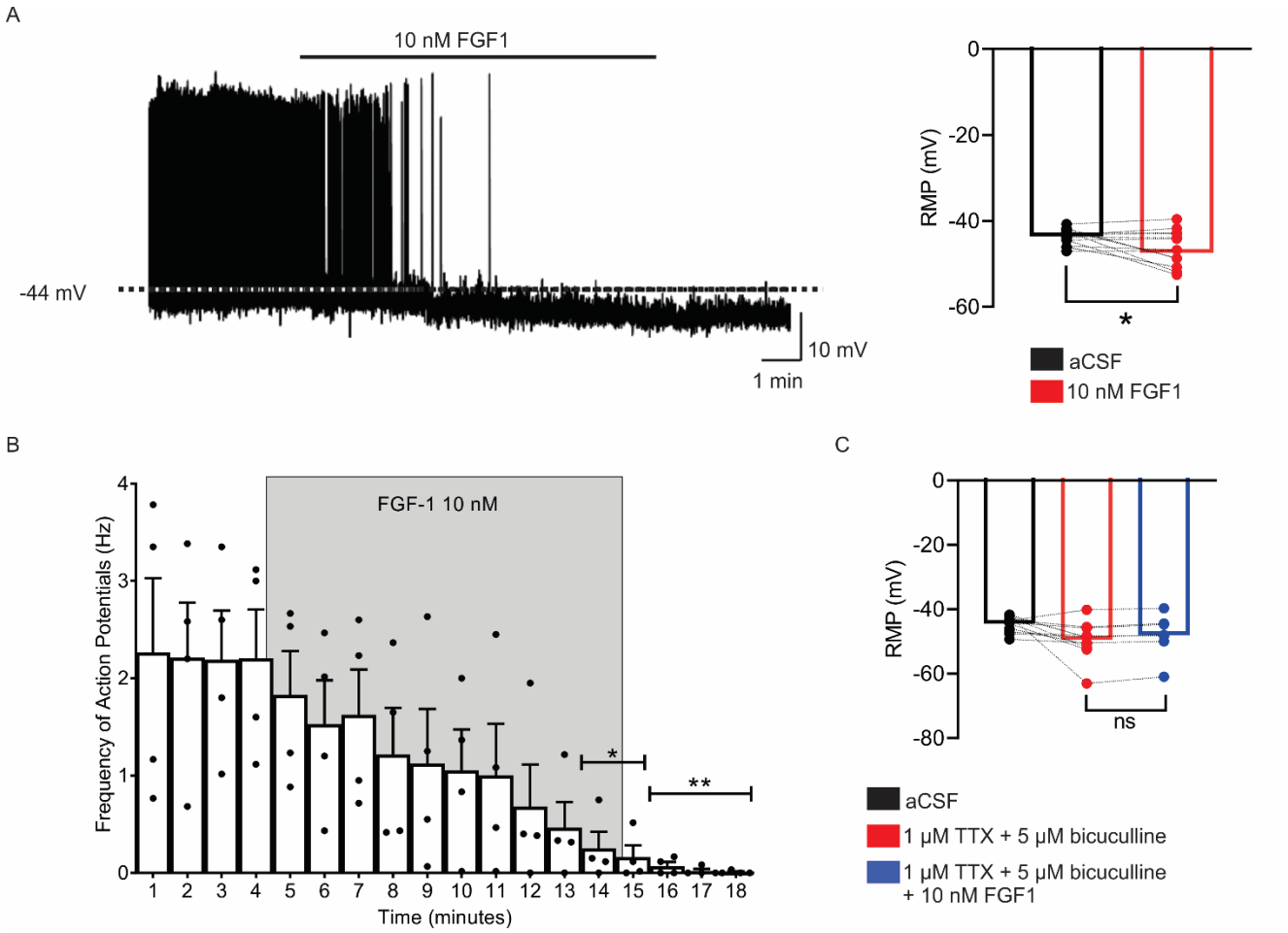

Figure 2. FGF1 inhibits NPY/AgRP neurons by an indirect mechanism. (A) Representative trace of an NPY/AgRP neuron illustrating a membrane hyperpolarization in response to FGF1 (10 nM). Bar graph shows the magnitude of FGF-1 responses in NPY/AgRP neurons. (B) FGF-1 (10 nM) decreased the action potential frequency in NPY/AgRP neurons progressively over a 10-minute period. (C) FGF-1 fails to change the membrane potential of NPY/AgRP neurons in the presence of TTX 1 μM, bicuculline 5 μM. Results are shown as mean ± SEM. *p<0.05 and **p<0.01, Statistics performed are as follows; For A: paired t-test. For B: ANOVA, Dunnett's multiple comparison. For C: ANOVA, Bonferroni correction as post hoc. Dashed line indicates the Resting Membrane Potential (RMP). 7 mice were used to generate data for Figures 2A (n=13) and 2B (n=4). 7 mice were also used to generate data from Figure 2C (n=7).

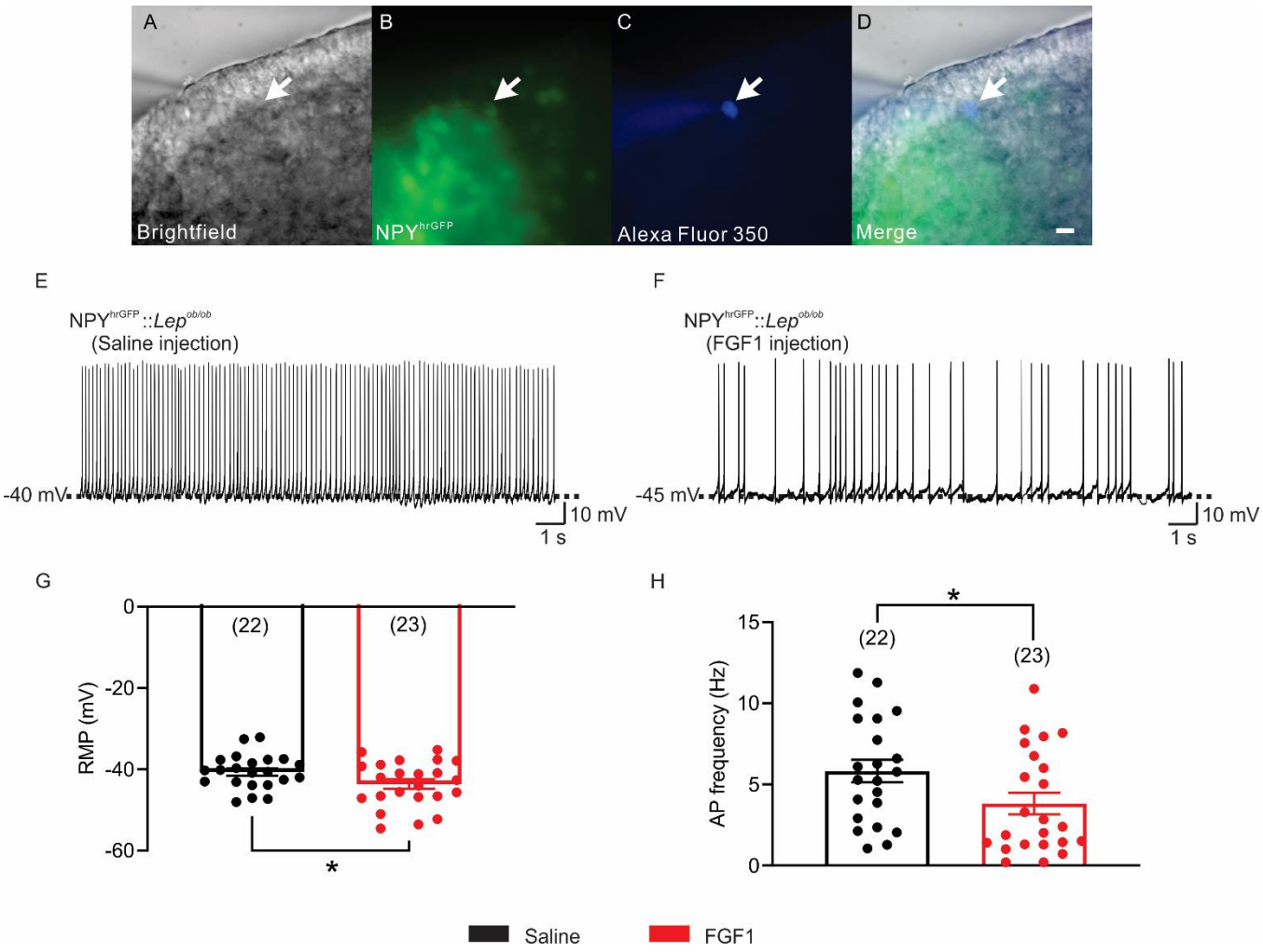

Figure 3. FGF1 persistently inhibits NPY/AgRP neurons in *Lep$^{ob/ob}$* mice. Brightfield illumination (A) of an NPY neuron from *Lep$^{ob/ob}$* mice. The same neuron under FITC (hrGFP; B) and Alexa Fluor 350 illumination (C). Merged image of targeted NPY neuron is shown in (D). Arrow indicates the targeted cell. Scale bar = 50 µm. Current-clamp recording of an NPY neuron shows the resting membrane potential from male *Lep$^{ob/ob}$* mice receiving saline (E) or FGF1 (F). Histograms demonstrate the average resting membrane potential (G) and action potential frequency (H) of NPY neurons from male *Lep$^{ob/ob}$* mice injected with saline (black; n=22, from 3 mice) or FGF1 (red, n=23, from 3 mice). Data are taken from NPY neurons of male NPY^{hrGFP}::*Lep$^{ob/ob}$* mice and are expressed as mean ± SEM. * $p<0.05$, unpaired t-test compared to Saline group. The number of neurons studied for each group is in parentheses.

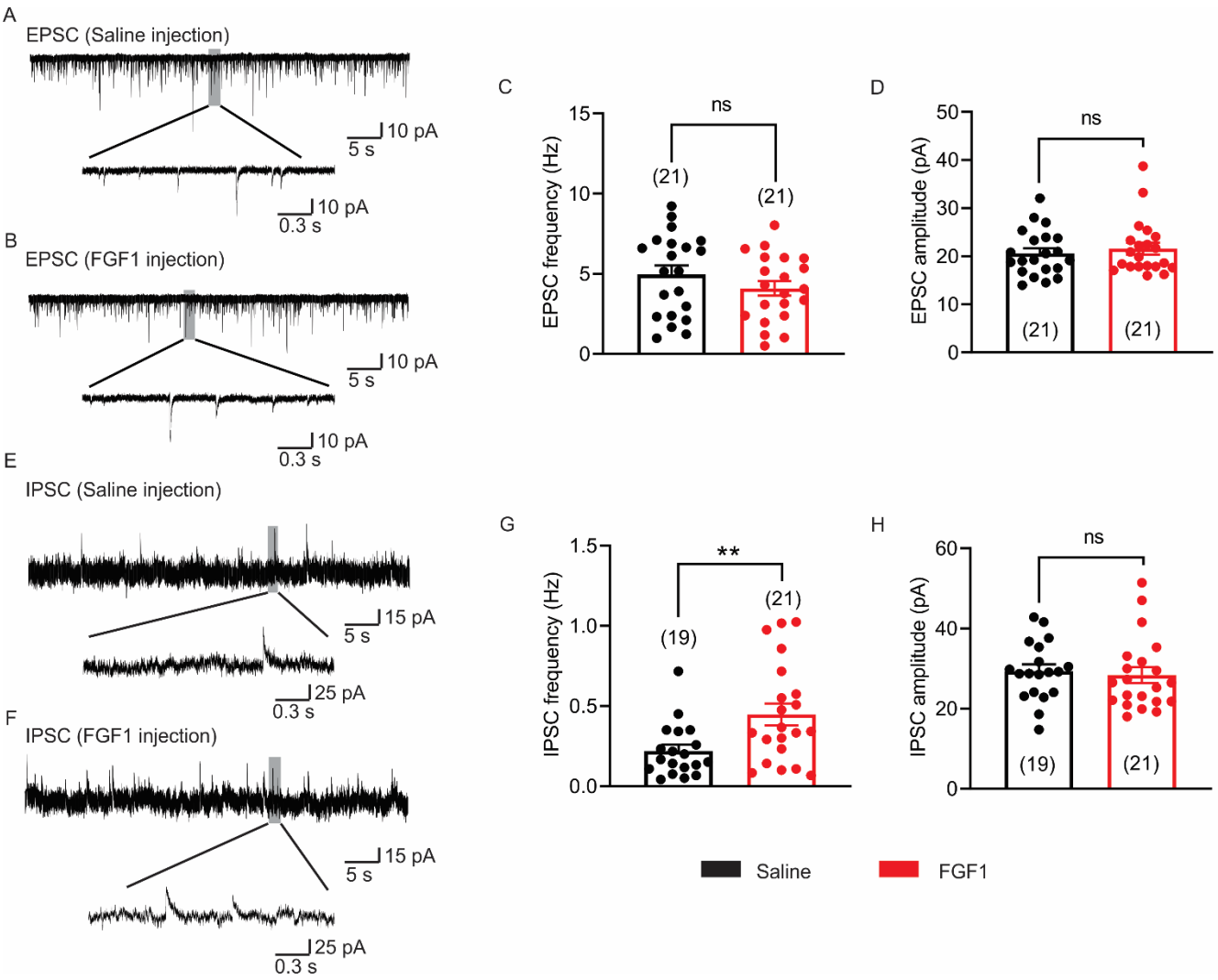

Figure 4. FGF1 enhances an inhibitory tone onto NPY/AgRP neurons in *Lep*$^{ob/ob}$ mice. Voltage clamp recording of excitatory postsynaptic currents (EPSCs) observed in arcuate NPY neurons from *Lep*$^{ob/ob}$ mice 2 wk after icv injection of either saline (A) or FGF1 (B). Histograms demonstrate the average EPSC frequency (C) and amplitude (D) of NPY neurons from male *Lep*$^{ob/ob}$ mice receiving icv saline (black; n=21, from 3 mice) or FGF1 (red; n=21, from 2 mice). Voltage clamp recording of inhibitory postsynaptic currents (IPSCs) observed in arcuate NPY neurons from *Lep*$^{ob/ob}$ mice after icv saline (E) or FGF1 (F) injection. Histograms demonstrate the average IPSC frequency (G) and amplitude (H) of NPY neurons from male *Lep*$^{ob/ob}$ mice receiving icv saline (black; n=19, from 3 mice) or FGF1 (red; n=21, from 2 mice) injection. Data are taken from NPY neurons of male NPY^{hrGFP}::*Lep*$^{ob/ob}$ mice and are expressed as mean ± SEM. ** p<0.01, unpaired t-test compared to Saline group. The number of neurons studied for each group is in parentheses.

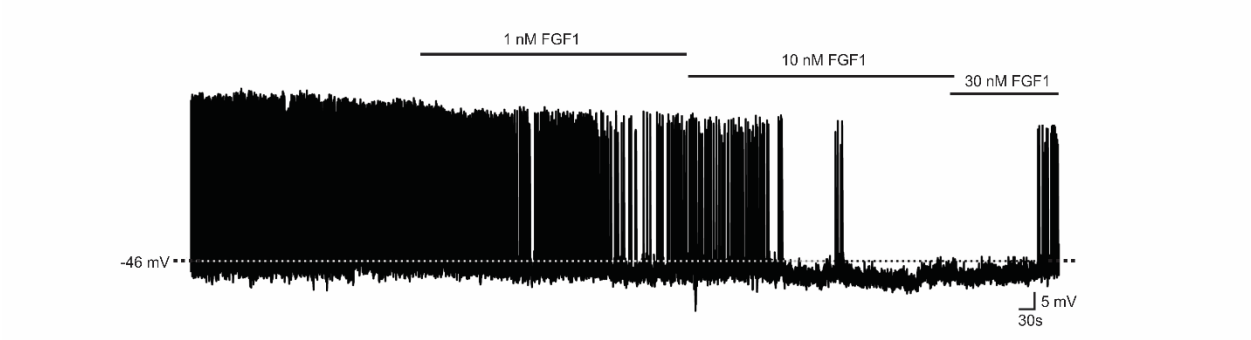

Supplementary figure 1 (related to Figure 2). FGF-1 reduced AP frequency of NPY/AgRP neurons in a concentration-dependent manner. Current clamp trace showing FGF-1 effects at 1, 10, and 30 nM in NPY/AgRP neurons (5 mice were used to generate data)**.**

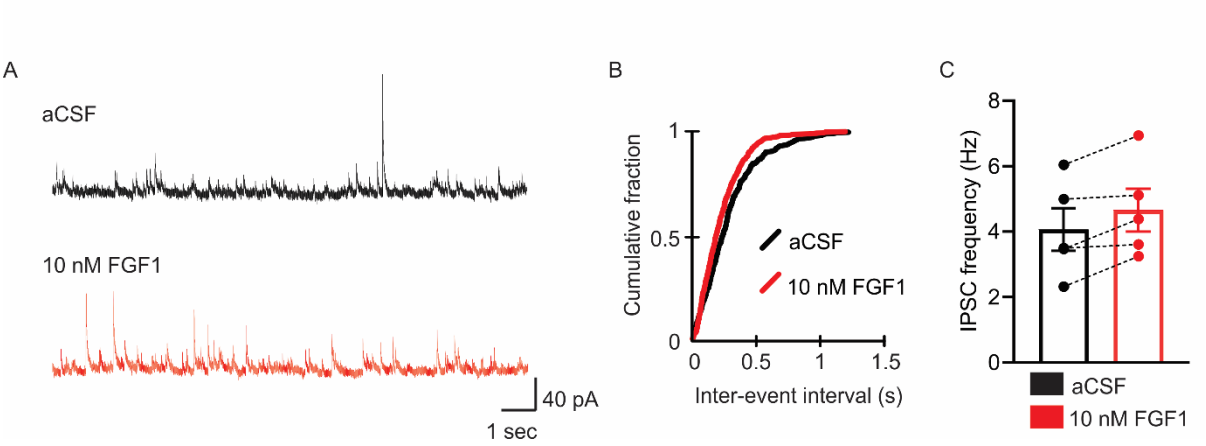

Supplementary figure 2 (related to Figure 2). Bath application of FGF1 enhances GABAergic tone onto NPY neurons in an ex vivo slice preparation. (A) Representative trace showing the spontaneous IPSC frequency of an NPY neuron before (black) and during (red) bath application of 10 nM FGF1. (B) Cumulative fraction plot shows a significant increase in sIPSC frequency in response to FGF1 (KS test; $P < 0.05$). (C) Histogram indicating FGF1-induced changes in sIPSC frequency observed in 5 neurons (from 4 slices in 1 mouse).

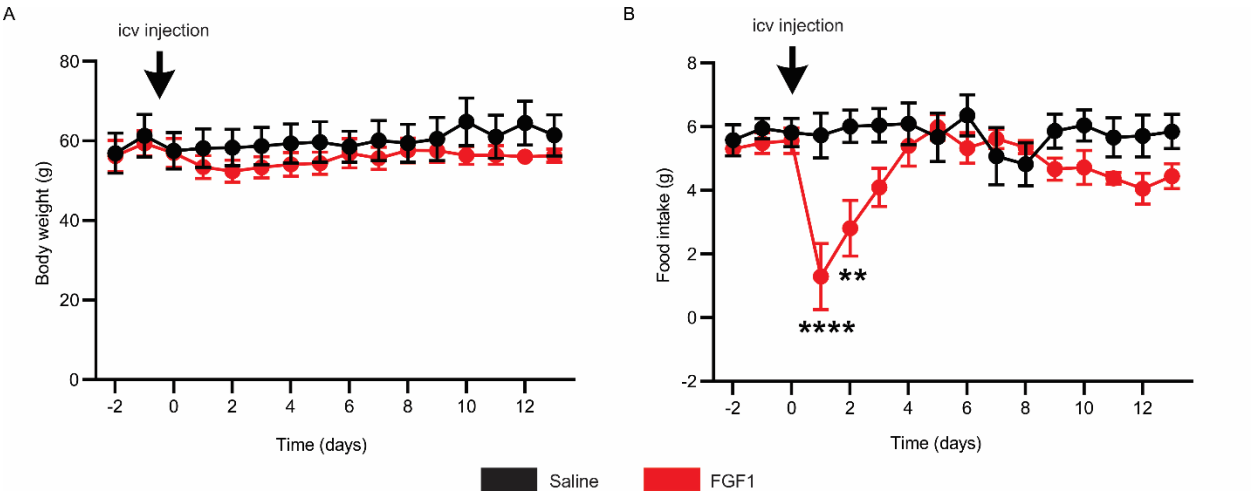

Supplementary figure 3 (related to Figures 3 and 4). A single injection of FGF1 (icv) transiently reduces food intake in *Lep*$^{ob/ob}$ mice. (A) Body weight curve and (B) food intake of male *Lep*$^{ob/ob}$ mice that received a single injection of FGF1 (red) or Saline (black) into the lateral ventricle. Data are from male *Lep*$^{ob/ob}$ mice (n=3-4) and are expressed as mean ± SEM. ** p<0.01 and **** p<0.0001, multiple unpaired t-test compared to Saline group.

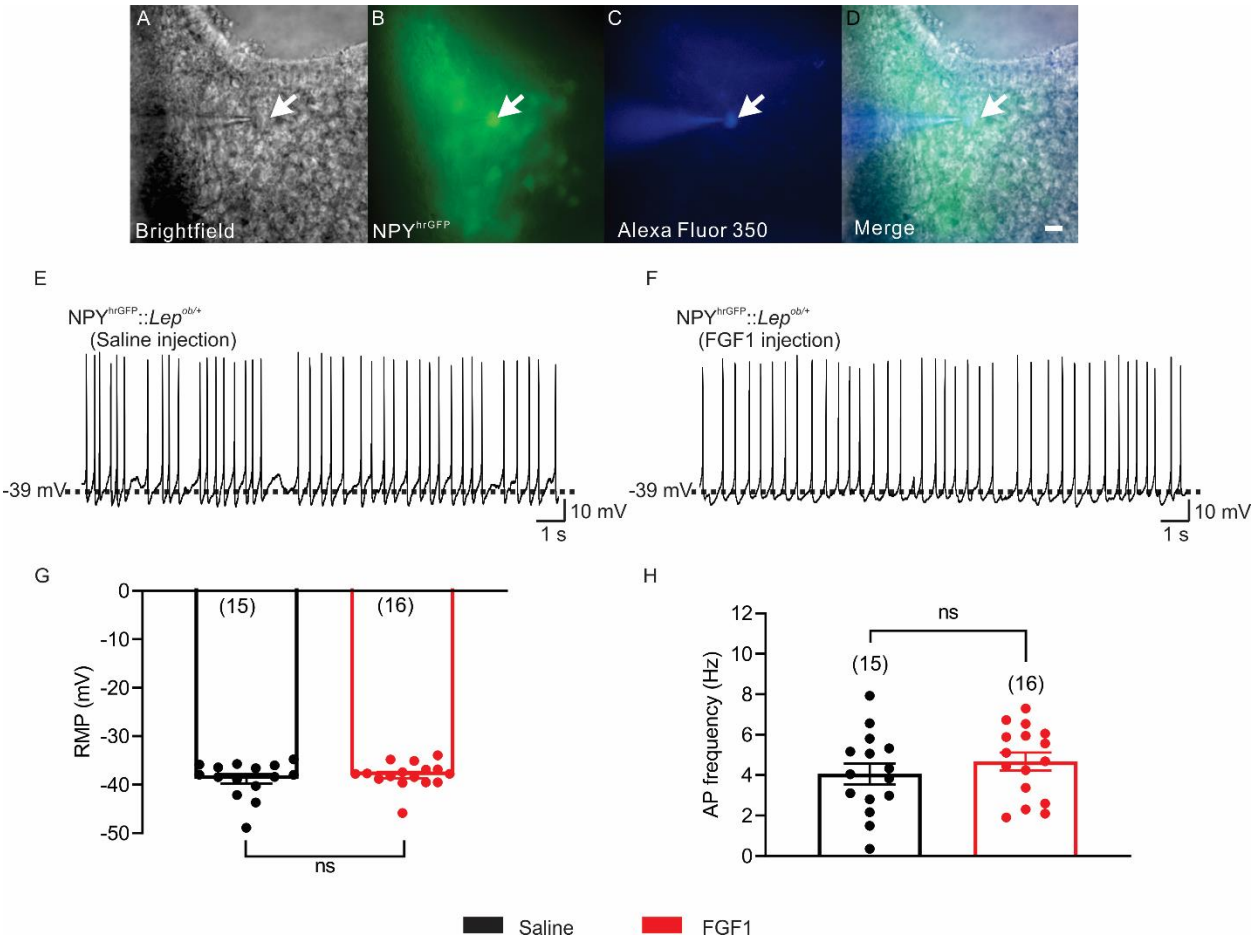

Supplementary figure 4 (related to Figure 3). NPY/AgRP neuronal activity from *Lep*$^{ob/+}$ mice remains unchanged 2 wk after icv injection of FGF1. Brightfield illumination (A) of NPY neurons from *Lep*$^{ob/+}$ mice. The same neuron under FITC (hrGFP; B) and Alexa Fluor 350 illumination (C). Merged image of targeted NPY neuron in shown in (D). Arrow indicates the targeted cell. Scale bar = 50 µm. Current-clamp recording shows the resting membrane potential of an NPY neuron from a male *Lep*$^{ob/+}$ mouse that received saline (E) or FGF1 (F). Histograms demonstrate the average resting membrane potential (G) and action potential frequency (H) of NPY neurons from male *Lep*$^{ob/+}$ mice following injection of saline (black; n=15, from 2 mice) or FGF1 (red; n=16, from 2 mice). Data are taken from NPY neurons of male NPY^{hrGFP}::*Lep*$^{ob/+}$ mice and are expressed as mean ± SEM. unpaired t-test compared to Saline group. The number of neurons studied for each group is in parentheses.

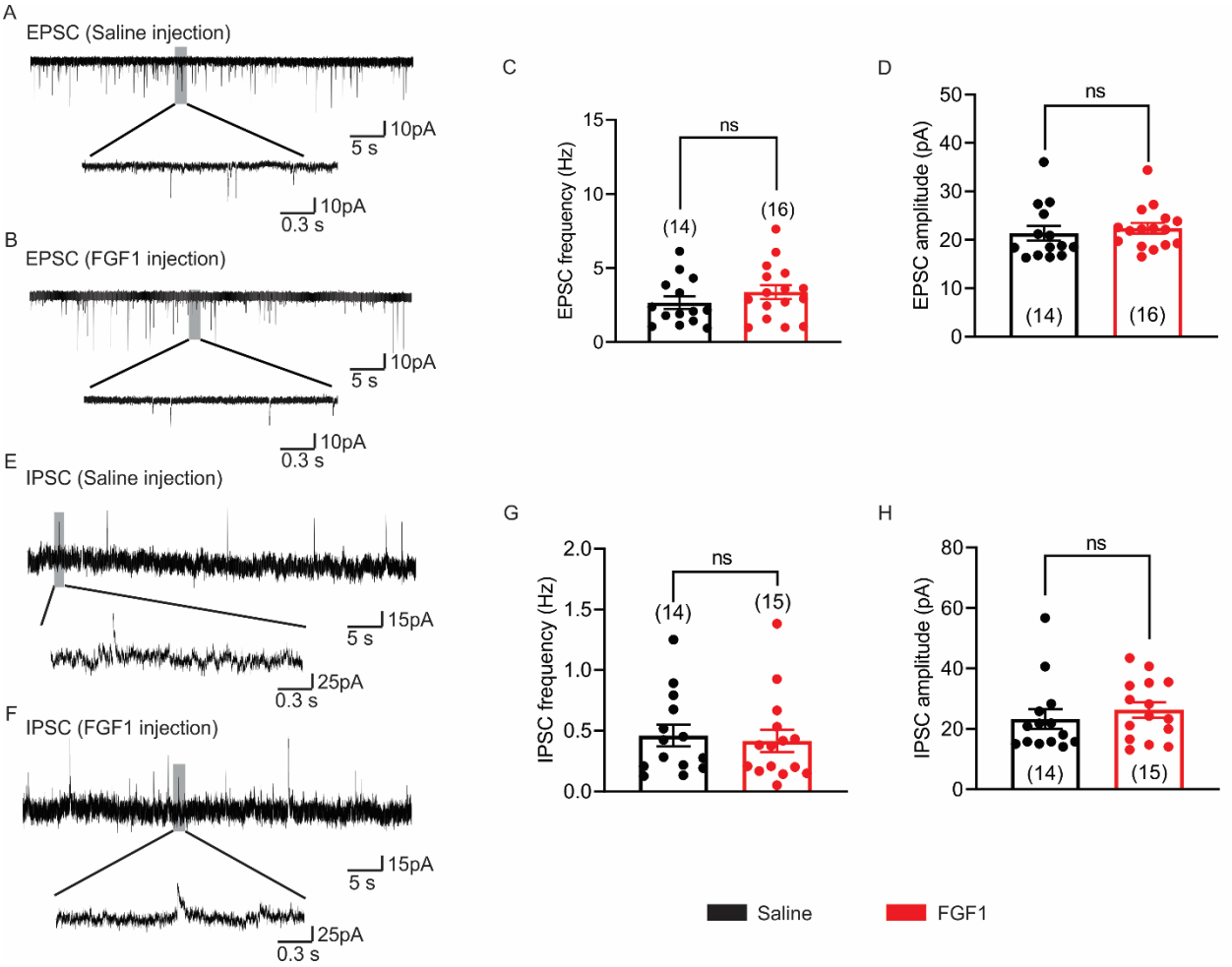

Supplementary figure 5 (related to Figure 4). Synaptic activity of NPY/AgRP neurons from *Lep*$^{ob/+}$ mice remains unchanged 2 wk after icv injection of FGF1. Voltage clamp recording of excitatory postsynaptic currents (EPSCs) observed in an NPY neurosn from *Lep*$^{ob/+}$ mice 2 wk after i.c.v. saline (A) or FGF1 (B) injection. Histograms demonstrate the average EPSC frequency (C) and amplitude (D) of NPY neurons from male *Lep*$^{ob/+}$ mice injected with either saline (black; n=14, from 2 mice) or FGF1 (red; n=16, from 2 mice). Voltage clamp recording of inhibitory postsynaptic currents (IPSCs) observed in an NPY neuron from *Lep*$^{ob/+}$ mice 2 wk after i.c.v. injection of saline (E) or FGF1 (F). Histograms demonstrate the average IPSC frequency (G) and amplitude (H) of NPY neurons from male *Lep*$^{ob/+}$ mice injected with saline (black; n=14, from 2 mice) or FGF1 (red; n=15, from 2 mice). Data are taken from NPY neurons

of male NPY^{hrGFP}::*Lep*$^{ob/+}$ mice and are expressed as mean ± SEM. unpaired t-test compared to Saline group. The number of neurons studied for each group is in parentheses.

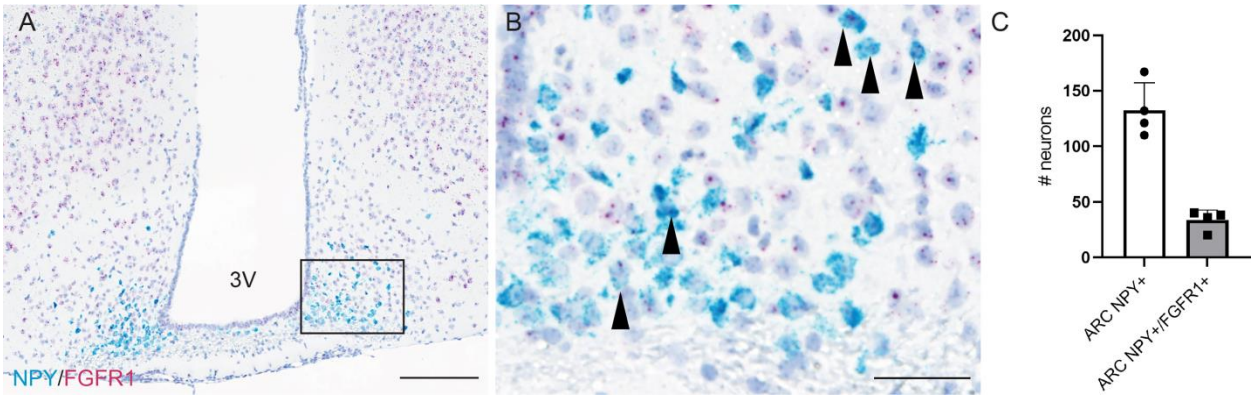

Supplementary figure 6. Co-expression of *FGFR1* mRNA in NPY neurons. A: Representative duplex ISH to *NPY* (teal) and *FGFR1* (red), with inset expanded in panel B. Arrows in panel B denote NPY neurons that contain *FGFR1* mRNA. C: <20% of NPY neurons (123/644, mean of 33.5 neurons per section) quantified in our analysis contain *FGFR1* mRNA whereas the majority of NPY neurons do not contain *FGFR1* mRNA (521/644 neurons, mean of 132.5 neurons per section). Data were analyzed from 2 hypothalamic sections from 2 separate mice. Scale bars in D = 200 µm, E = 50 µm.